Separation and Purification Technology 377 (2025) 134347

Contents lists available at ScienceDirect

Separation and Purification Technology

journal homepage: www.elsevier.com/locate/seppur

Biochar-based Downflow Fixed-Bed Adsorption Systems for Water Treatment: Process Optimization, Reusability, and Techno-Economic Evaluation

Oussama Baaloudj [a,*], Fausto Langerame [a], Rocco Iunnissi [b], Gianluigi Buttiglieri [c], Daniele Del Buono [d], Samia Khadhar [e], Laura Scrano [a], Vincenzo Trotta [f,g], Monica Brienza [a,*]

[a] Department of Basic and Applied Sciences (DiSBA), University of Basilicata, via dell'Ateneo Lucano 10, 85100 Potenza, Italy
[b] Agenzia Regionale per la Protezione dell'Ambiente della Basilicata (ARPAB), Sede Centrale: Via della Fisica, 18 C/D, 85100 Potenza, Italy
[c] Catalan Institute for Water Research (ICRA-CERCA), C. Emili Grahit 101, 17003 Girona, Spain
[d] Department of Agricultural, Food and Environmental Sciences, University of Perugia 06121 Perugia, Italy
[e] Laboratory of Georesources, Technopole of Borj Cedria, University Carthage, Soliman, Tunisia
[f] Department of Agricultural Forestry, Food and Environmental Sciences (DAFE), University of Basilicata, Potenza, Italy
[g] BioPlanEU, srls, Via dei Molinari 144, 85100 Potenza, Italy

ARTICLE INFO

Editor: Dr Philiswa Nomngongo

Keywords:
Adsorption
Cost-effective treatment
Fixed-bed column
Surface Water
Wastewater
Regeneration

ABSTRACT

Adsorption processes have emerged as promising solutions for water treatment, particularly when utilizing bioderived materials, due to their environmental sustainability. Nevertheless, a key challenge of this approach lies in the regeneration of spent materials. This study investigates the possibility of using biochar in a fixed-bed adsorption system for water treatment, focusing on its potential reuse following an environmentally friendly regeneration process and evaluating its feasibility for large-scale applications. Rapid small-scale column tests were conducted to optimize process parameters for removing sulfamethoxazole while using a high concentration to prove the concept and evaluate process efficiency. Under optimal conditions, the column maintained its operational capability after treating 33 L, achieving a saturation time of up to 130 h. The adsorption behavior was explored using kinetic models, analyzing breakthrough curves to reveal dynamic performance. The Clark model demonstrated the highest degree of fit to the data, making it a reliable tool for predicting adsorption efficiencies. The reusability of the adsorbent was evaluated through a sustainable regeneration approach, enabling effective reusability for up to 5 cycles. The applicability of the proposed treatment method was further validated on real water samples, demonstrating a significant reduction in turbidity and the concentration of detected substances in the samples. Finally, a techno-economic assessment estimated a treatment cost of €0.89/m^3, supporting the economic feasibility of the approach. This research highlights the efficiency and scalability of the proposed process as a viable, cost-effective water treatment solution for large-scale applications.

1. Introduction

Ensuring clean and uncontaminated water resources is essential for environmental safety and public health; however, most water sources are increasingly contaminated by various emerging contaminants (ECs), which include pharmaceuticals [1,2]. Antibiotics, in particular, are consistently being detected in wastewater and surface waters at concentrations ranging from nanograms to micrograms per liter [3,4]. Among antibiotics, sulfamethoxazole (SMX), a widely used sulfonamide in human and veterinary therapy, has the potential to bioaccumulate throughout the food chain, resulting in detrimental effects for ecosystems [5], non-target organisms [6], and humans [7]. In addition, exposure to SMX raises concerns about public health due to the development of antibiotic resistance [8].

Recent research focuses on optimizing the removal of various contaminants from water using different advanced processes [9,10]. However, while effective in theory, many of these methods face challenges in scaling, making them difficult to implement due to high costs [11] and limited flexibility [12]. Alternatively, adsorption-based materials provide a practical and cost-effective method for water treatment,

* Corresponding authors.
E-mail addresses: Oussama.baaloudj@unibas.it (O. Baaloudj), Monica.brienza@unibas.it (M. Brienza).

https://doi.org/10.1016/j.seppur.2025.134347
Received 9 March 2025; Received in revised form 22 May 2025; Accepted 13 July 2025
Available online 14 July 2025

efficiently removing ECs from wastewater [13]. Their use in remediation strategies offers flexibility, as the wide variety of available adsorbents allows for cost reduction based on optimized material selection [14]. One of the most economical and sustainable approaches to developing eco-friendly and effective adsorbents is through waste valorization. This approach not only mitigates waste accumulation but also enables the production of bio-based adsorbents that effectively remove pollutants from water, aligning with the principles of the circular economy [15]. In this context, a strategic method for producing adsorbent material is the application of pyrolytic processes to waste [16]. Among the bio-waste sources available, forest residues from wood harvesting offer a promising supply of lignocellulosic material that is abundant, readily accessible, and can be converted into effective biochar adsorbents [17].

Biochar is a low-cost material that can effectively remove ECs and other pollutants from greywater, wastewater, and surface water [18], due to its distinctive properties, including a large specific surface area, multiple functional groups, and broad sorption sites [19–21]. Thus far, the majority of biochar applications for pollutant removal have been conducted on batch adsorption [14,22], as also reported in our previous study, which demonstrated its efficacy in eliminating four different pollutants [23]. While batch experiments are crucial for assessing adsorption characteristics, such as removal mechanisms, they are limited in practical applicability, as they do not provide data directly applicable to large-scale treatment systems [24,25]. In contrast, continuous adsorption column systems offer promising potential due to their scalability, ranging from small-scale setups to large industrial applications [26–28].

Column systems follow two configurations, depending on the specific experimental objectives and application type, namely down-flow (DoF) and up-flow (UpF). Although both configurations are assumed to produce similar behaviors due to their similar mechanisms, their efficiency may differ due to multiple factors [29]. UpF improves system adsorption efficiency by slightly elevating the adsorbent bed, which reduces channeling and extends contact time between pollutants and adsorbent [30]. However, the UpF configuration is less prevalent in wastewater treatment compared to the widely used DoF configuration, due to DoF's ability to better simulate large-scale systems, its low hydraulic pressure demands for water flow, and its capability to facilitate single-step adsorption while averting particle accumulation at the bed's base [31,32].

This study investigated the feasibility of using biochar in a DoF fixed-bed adsorption system for water treatment through Rapid Small Scale Column Tests (RSSCTs), which provide a quicker and more efficient approach for predicting the performance of pilot-scale systems [33,34]. Process parameters, including flow rate and bed length, were optimized to maximize SMX removal while applying a high concentration in this step to prove the process concept and evaluate process efficiency. Breakthrough curves and adsorption behavior were analyzed using kinetic models. The system's reusability was evaluated through a novel continuous regeneration method, while its real-world applicability was validated with treatment tests on real water samples. Finally, a techno-economic assessment was conducted to determine the feasibility of the system. To our knowledge, no studies have been conducted utilizing this setup to remove antibiotics from water using biochar. Moreover, the use of the proposed dual-column biochar adsorption system that sustainably treats water and regenerates biochar simultaneously has never been proposed. Finally, biochar application for treating real wastewater and surface water in downflow continuous adsorption has not been investigated yet.

2. Materials and methods

2.1. Chemical reagents

The chemicals used in this study were analytical grade. SMX ($C_{10}H_{11}N_3O_3S$, purity > 98 %) and sodium persulfate ($Na_2S_2O_8$, purity ≥ 99.0 %) were supplied by Sigma-Aldrich®. A Millipore Milli-Q system was used to purify ultrapure water (18.3 MΩ cm) from Billerica, Massachusetts, USA. HPLC/MS grade of water, acetonitrile, and methanol were also obtained from Sigma-Aldrich®. For SMX adsorption studies, a 1,000 mg/L stock solution was prepared in methanol and stored at 4 °C. After that, working solutions with an SMX concentration of 5 mg/L to test the performance of the system were prepared by diluting the stock solution in distilled water and stored in a glass tank. Real water samples, including wastewater and surface water, were collected from various locations in the Basilicata region, southern Italy. Wastewater samples were taken from the outlet of a secondary wastewater treatment plant, while surface water samples were collected from a city river and a dam.

2.2. Adsorbent

The biochar used in this study was the commercial product Crescifertilis (supplied by Terra Fertilis®, Caen, France). The biochar was obtained by pyrolyzing at 600 °C wood pellets from forest thinning operations obtained from Andaines Forest, Argentan, Orne 61, France. The composition and technical characteristics of the Crescifertilis biochar are presented in Tables SM1 and SM2 in the supplementary materials (SM).

2.3. Rapid small-scale column tests and analysis methods

The rapid small-scale column tests were performed in glass columns (internal diameter of 2.5 cm, length of 17 cm). The column was filled with a predefined quantity of biochar, and layers of granular particle stones were placed to prevent the leakage of biochar particles at both the bottom and top of the column while ensuring an equal flow velocity distribution. The inlet solution was circulated downward using a peristaltic pump with controlled flow. For optimization trials, an SMX solution (5 mg/L) was prepared by diluting a 1,000 mg/L stock solution in water at room temperature (20 °C) and neutral pH. The diluted solution was passed through the column while varying the bed depth and height (corresponding to a biochar mass of 10–23 g to ensure saturation) and adjusting the flow rate between 8.5 and 20 mL/min. For the real cases (surface and wastewater), the samples were passed through the column under optimal conditions. The experimental setup for adsorption in a fixed-bed column is illustrated in Fig. 1, while photographs of the setup and column are provided in Figure SM1.

The efficiency of the process was evaluated by monitoring pollutant concentrations before and after treatment. For optimization trials, SMX concentrations were analyzed using high-performance liquid chromatography (HPLC) (Agilent Technologies® 1200 Series) coupled with an ultraviolet (UV) detector, with analysis details presented in Table S3. The limits of detection (0.48 mg/L) and quantification (0.16 mg/L) were determined via calibration curve regression, as shown in Figure SM2. For real water applications, a non-target screening method was employed, utilizing solid-phase extraction (HLB Oasis, 6 cc, 500 mg), followed by measurement via UHPLC$^+$focused-MS/MS (Dionex Ultimate 3000 RS Column Comportament-Thermo Scientific Q Exactive Focus). The first 500 mL of surface water and 250 mL of wastewater were screened using a protocol similar to that reported in previous work [35], with analysis details presented in Table S4. The turbidity of the real water samples was measured using a turbidity meter (Hanna Instruments, model HI83414).

2.4. Adsorption modeling

In the fixed-bed analysis, the collected breakthrough curve data were modeled using four models (Equations (1) to (4) in their linear form to assess the column behavior, efficiency, and applicability in large-scale operations and the parameters controlling the adsorption performance [36].

Adams-Bohart Model [37,38]:

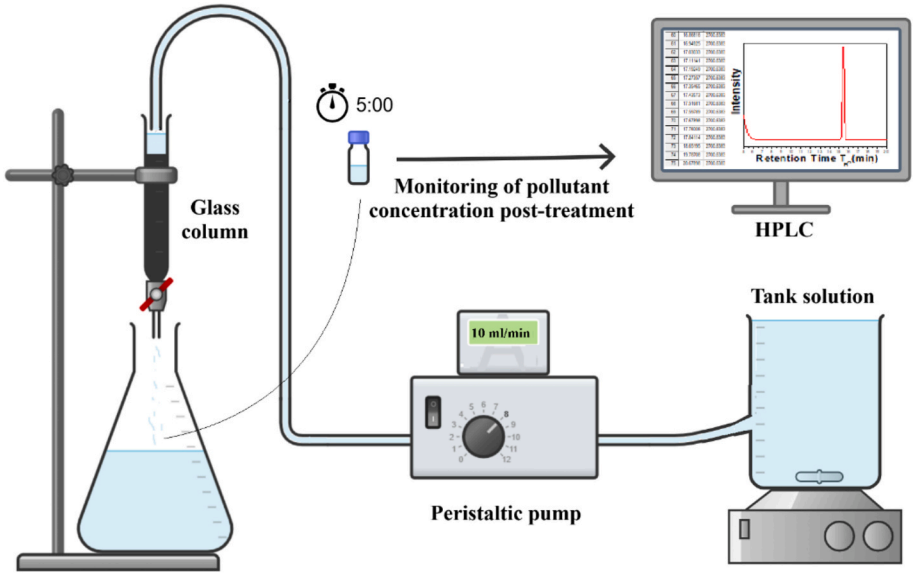

Fig. 1. Illustration of the fixed-bed column adsorption setup.

$$\frac{C}{C_o} = \exp\left(k_{AB}\, C_o t - k_{AB} N_o \frac{Z}{U_o}\right) \quad (1)$$

Thomas Model [34]:

$$\frac{C}{C_o} = \frac{1}{1 + \exp\left(-k_{TH}\, C_o t + k_{TH} q_o \frac{m}{Q}\right)} \quad (2)$$

Yoon-Nelson Model [39]:

$$\frac{C}{C_o} = \frac{\exp(k_{YN} t - \delta k_{YN})}{1 + \exp(k_{YN} t - \delta k_{YN})} \quad (3)$$

Clark Model [40]:

$$\frac{C}{C_o} = \left(\frac{1}{1 + A\exp(-r\,t)}\right)^{\frac{1}{n-1}} \quad (4)$$

Where: C_0 is the influent (inlet) concentration (mg/L), C is the effluent (outlet) concentration (mg/L), k_{AB} (L/mg × h) is the kinetic constant of the Adams-Bohart model, N_0 (mg/L) is saturation concentration, Z (cm) is the bed high or depth, U_0 (cm/h) is superficial velocity, k_{TH} (mL/h × mg) is Thomas model rate constant, q_0 (mg/g) is adsorption capacity, m (g) is adsorbent mass in the column, Q (mL/h) is volumetric flow rate, δ (h) is the time corresponding to 50 % adsorption, k_{YN} (h^{-1}) is Yoon-Nelson model rate constant, A is Clark model constant, r (mg/L × h) is adsorption rate and n is Freundlich adsorption constant.

The following formula can be used to determine the surface velocity U_0:

$$U_o = \frac{Q}{A} \quad (5)$$

Where: Q (mL/h) is the flow rate; A (cm^2) is the adsorption column's cross-sectional area which is a cylindrical column, and the value was calculated based on internal diameter (2.5 cm) to be 4.91 cm^2.

By simplifying its assumptions and focusing on the relationship between bed depth and service time at a specific breakthrough point, the Adams-Bohart model can be transformed into a practical approximation for scaling adsorption systems based on breakthrough performance, known as the Bed Depth Service Time (BDST) model (Equation (6) [41,42].

$$t = \frac{N_o}{C_o\, U_o} Z - \frac{1}{K_0\, C_o} \ln\left(\frac{C_o}{C} - 1\right) \quad (6)$$

2.5. Regeneration of adsorbent

The continuous regeneration method using thermally activated persulfate (PS) was employed to regenerate the column, as previous investigations have demonstrated its sustainability and efficiency compared to other methods [23], resulting in a sustained post-adsorption step and regeneration process that prevents saturation and mitigates the risk of contaminants in the saturated biochar. For each regeneration step, 1 L of the regenerating solution was passed through the column at a flow rate of 8.5 mL/min, with the optimal PS concentration previously determined as [PS] = 20 mM [43]. The temperature for activation was set to 60 °C, which was identified as the optimal value in earlier studies [44]. Following regeneration, the column was washed with 2 L of water at a flow rate of 16 mL/min and then dried before being reused in adsorption experiments. The efficiency of regeneration was quantified across cycles based on adsorption efficiency, as determined using the equation below:

$$\text{Adsorption efficiency}\,(\%) = \frac{(C_o - C)}{C_o} \times 100(\%) \quad (7)$$

The concentration of adsorbed SMX was assessed by desorbing the adsorbed SMX in 2 g of biochar using 100 mL of a solution containing 1 M sodium hydroxide (NaOH) and methanol (9:1 v/v ratio) under ultrasonic conditions for 30 min [43]. The experiment was run in triplicate, and the solutions were analyzed via HPLC. Additionally, these trials helped determine whether SMX degradation occurred during the regeneration process.

2.6. Characterization of adsorbent

The biochar was characterized before adsorption, after adsorption, and during regeneration using different characterization techniques. The SEM XL30 ESEM PHILIPS FEI equipment was employed to analyze morphology. The Raman spectra were obtained using a LabRam (Horiba-JobinYvon) spectrometer, equipped with an edge filter, two diffraction gratings (600 and 1,800 grooves/mm), and an Olympus microscope. The spectrometer was connected to a CCD detector cooled to −70 °C via the Peltier effect to ensure optimal signal detection. A He-Ne laser (λ = 632.8 nm, 20 mW) served as the laser source, with intensity carefully controlled using a neutral density filter carousel to prevent sample degradation. The X-ray photoelectron spectroscopy (XPS) spectra of the studied materials were obtained using a SPECS

spectrometer (Phoibos 100-MCD5) at 10 kV and 10 mA in a medium area (diameter = 2 mm) with the MgKα (1253.6 eV) source operating under chamber pressure below 10^{-9} mbar. The acquired XPS spectra were analyzed using the curve-fitting program (NewGoogly). Peak positions (binding energies, BEs) derived by the curve-fitting are referenced to C1s aromatic carbons as the internal standards set at 284.3 eV.

3. Results and discussions

3.1. Optimization and modeling of adsorption

Flow rate and bed depth (Z) are essential factors for assessing the efficacy of an adsorption process, especially for the continuous treatment of wastewater on a large scale. The adsorption trials were studied as a function of time to explore breakthrough curves. Starting with the flow rate, Fig. 2(a) shows its effect on system efficiency during the first 5 min. The data show that decreasing the solution flow rate improves system efficiency by increasing contact time with the adsorbent. Only a small variation in adsorption efficiency was observed between flow rates of 8.5 and 10 mL/min, which can be considered negligible.

The bed depth experiments were initially investigated using the BDST model to calculate sorption capacities and kinetic constants. The service times ($C/C_0 = 0.80$, $C/C_0 = 0.55$, $C/C_0 = 0.30$) for bed depths of 5.5, 9, and 12.5 cm at a constant flow rate of 10 mL/min and an initial concentration of 5 mg/L were determined. Fig. 2 (b) illustrates the relationship between service time *vs* bed depths modeled with the BDST model. The model parameters, calculated from the slope and intercept, are shown in Table 1. The high R^2 values confirm the reliability of this model in predicting adsorption performance at different bed depths in continuous columns.

The effects of bed height and depth on the breakthrough curve were also investigated under identical conditions. Fig. 3 illustrates the breakthrough curves for bed depths (biochar mass) of 5.5 cm (10 g), 9 cm (16.5 g), and 12.5 cm (23 g). The results show that increasing bed depth enhances column performance by extending breakthrough and saturation time. The column with a 12.5 cm bed depth continued to operate even after treating 33 L of 5 mg/L SMX, reaching an 80 % saturation rate, and demonstrating its ability to function for up to 130 h before complete saturation. The improved adsorption performance with increasing bed depth is attributed to a greater number of adsorption active sites in the adsorbent and the longer contact time between the pollutant and biochar [45].

The breakthrough curves were fitted to various models to describe the fixed-bed column kinetics, as shown in Fig. 4. The high R^2 values indicate a strong fit between the experimental data and the tested model, suggesting their potential applicability for describing the adsorption process in this column. The parameters for all models are summarized in Table 2.

Fig. 4 (a) presents the Adams-Bohart model, showing that as bed depth increases, the Adams-Bohart kinetic constant (k_{AB}) decreases, resulting in a rise in saturation concentration N_o, due to the greater availability of adsorption sites in the column [46]. Thomas's modeling (Fig. 4 b) indicates that internal and external diffusion are not limiting steps in the adsorption process [47]. The Thomas constant (k_{TH}) decreases with increasing bed depth, while adsorption capacity (q_o) increases, corresponding to an increased number of available adsorption sites [48]. Fig. 4 (c) shows the Yoon-Nelson model, which estimates the time required for 50 % adsorption (δ). The results show that δ increases with bed depth, while the Yoon-Nelson constant (k_{YN}) decreases. Clark's model combines the Freundlich isotherm with mass transfer theory. To

Table 1
Bed depth service time model parameters.

C/C_0	N_0 (mg/L)	K_0 (L/mg)	Z_0 (cm)	R^2
0.8	71.4	−0.009	4.57	0.998
0.55	20.4	−0.004	5.67	0.804
0.33	2.19	0.187	3.56	0.929

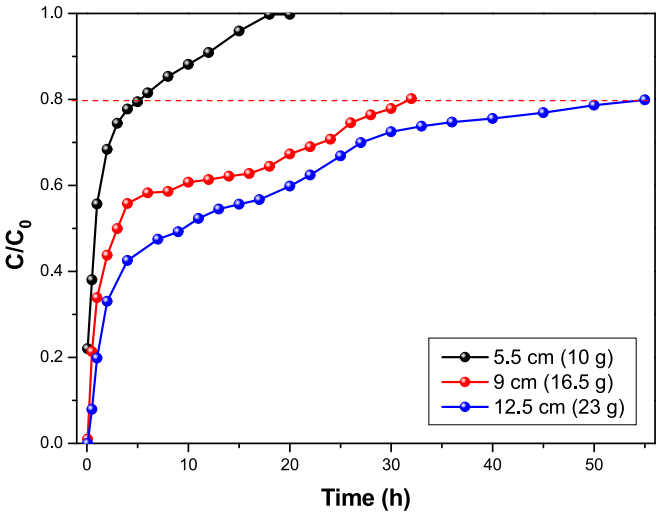

Fig. 3. Breakthrough curves for different bed depths with a flow rate of 10 mL/min.

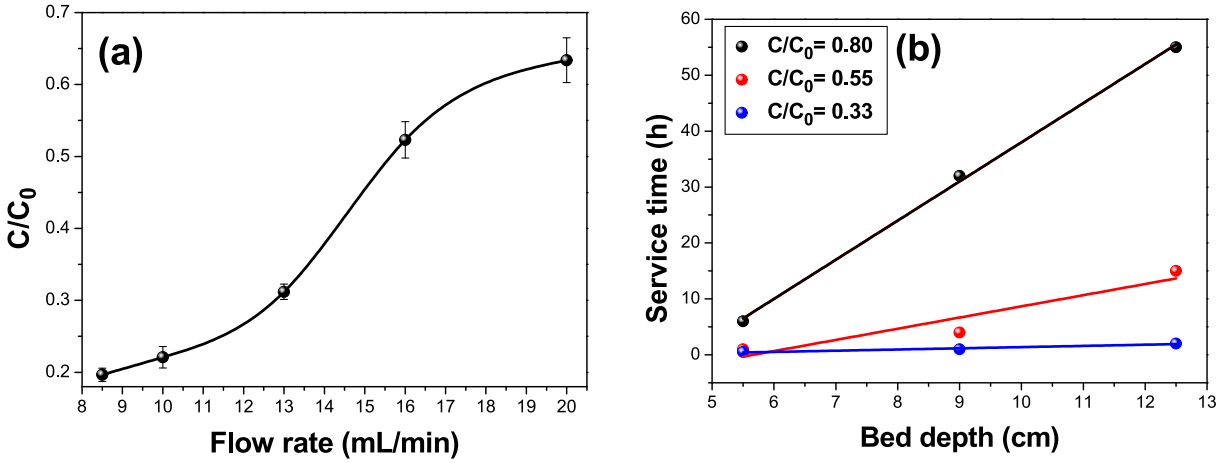

Fig. 2. **(a)** Effect of flow rate on the efficiency of the column in the first 5 mins, bed depth 5.5 cm, **(b)** Bed depth service time model fitting curve for SMX removal, flow rate 10 mL/min.

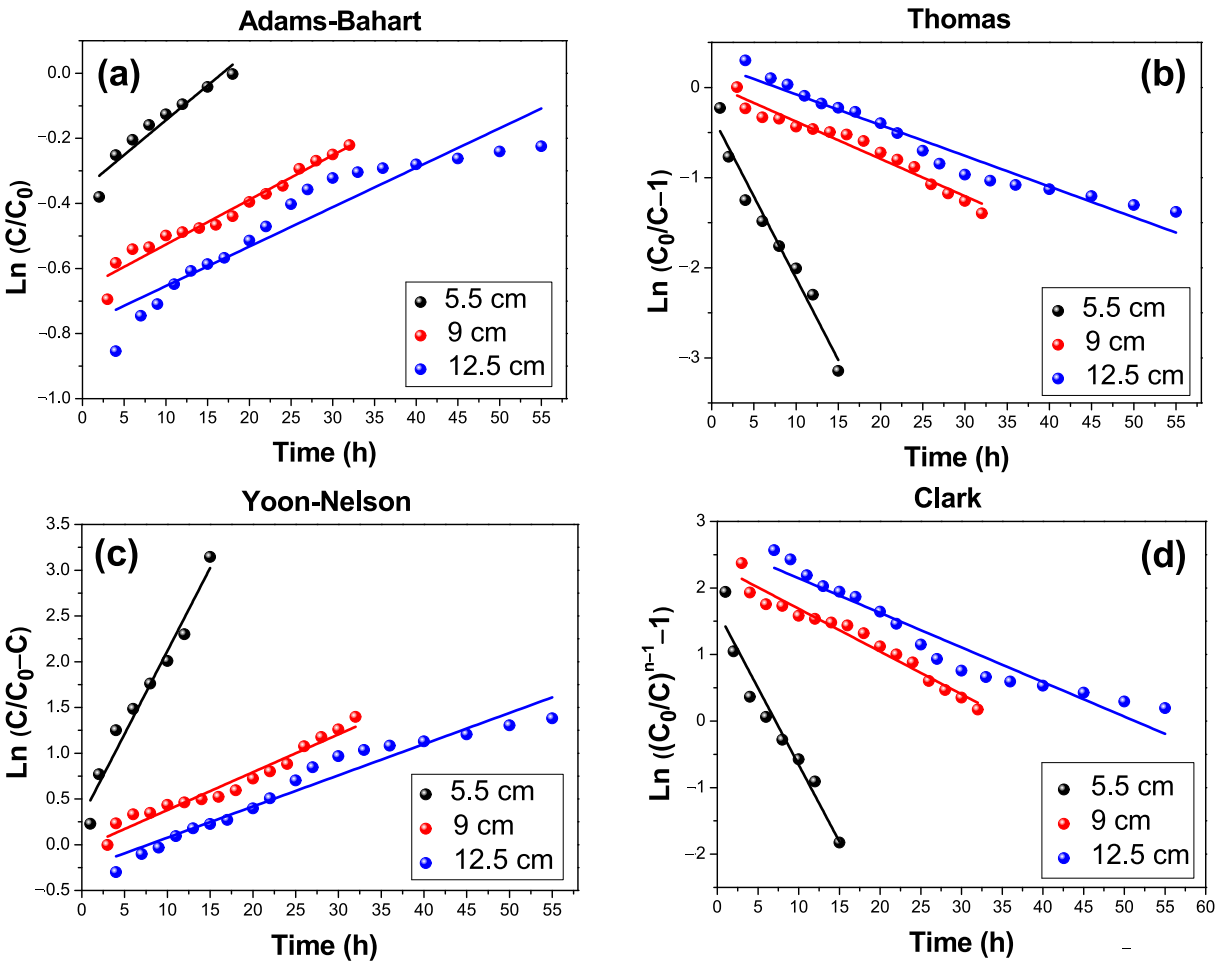

Fig. 4. Linear modeling of the breakthrough curve for SMX removal at different depths, **(a)** Adams-Bahart, **(b)** Thomas, **(c)** Yoon-Nelson, and **(d)** Clark.

Table 2
Parameters of the Adams-Bohart, Thomas, Yoon–Nelson, and Clark breakthrough curve models.

	Bed depth (cm)	**k_{AB} (mL/mg × h)**	**N_o (mg/L)**	**R^2**
Adams-Bohart	5.5	0.004	33.17	0.917
	9	0.003	50.08	0.958
	12.5	0.002	63.25	0.883
	Bed depth (cm)	**k_{TH} (mL/h × mg)**	**q_o (mg/g)**	**R^2**
Thomas	5.5	0.030	2.84	0.845
	9	0.008	4.25	0.955
	12.5	0.006	38.75	0.943
	Bed depth (cm)	**k_{YN} (h^{-1})**	**δ (h)**	**R^2**
Yoon-Nelson	5.5	0.267	0.569	0.835
	9	0.041	0.851	0.955
	12.5	0.034	7.751	0.943
	Bed depth (cm)	**r (mg/L × h)**	**A**	**R^2**
Clark	5.5	0.231	5.215	0.936
	9	0.064	10.263	0.960
	12.5	0.052	14.392	0.919

apply the Clark model, the Freundlich isotherm parameter (n) must be determined; in this study, a value of 4.543 from previous research [23] was used. Fig. 4(d) demonstrates that all depth experiments fit well with this model. Notably, the data revealed that increasing bed depth slows the adsorption rate (r), extending the time to reach saturation. This trend also leads to an increase in the Clark model constant (A).

3.2. Regeneration of adsorbent

SMX interacts with the active adsorbent sites in biochar through chemical and physical interactions with its surface [49]. Consequently, the adsorbent gradually loses active sites with each regeneration cycle. To mitigate this, biochar regeneration using advanced oxidation processes was applied for SMX removal, based on previous batch adsorption studies [23]. Fig. 5 (a) illustrates the adsorption efficiency during the first five minutes of each regeneration cycle, while the kinetics are depicted in Figure SM3. Regeneration efficiency improved in the second cycle (82 %) compared to the first (77 %). Consequently, the adsorbent maintained or even exceeded its pre-regeneration SMX removal capacity, likely due to biochar surface modifications. In addition, saturation time after regeneration did not increase, possibly due to larger pores formed through surface modification, facilitating faster adsorption. After five cycles, the biochar retained 60 % efficiency, suggesting high regeneration potential and preservation of adsorption sites.

The concentration of SMX was measured in both the solution and biochar, along with PS concentration in the solution before and after heating, to determine whether the regeneration method degraded SMX or just desorbed it. The results are summarized in Fig. 5 (b). The PS concentration in the solution, determined using a method from the literature [50], decreased from 20 mM to 0 after heating, confirming its full activation to produce sulfate radicals ($SO_4^{\bullet-}$) and hydroxyl radicals ($^{\bullet}OH$). The concentration of SMX was then analyzed after passing the regenerating solution through the column. HPLC detected no SMX in the solution, thus pointing out complete SMX degradation. Additionally, SMX concentration on the biochar decreased significantly after

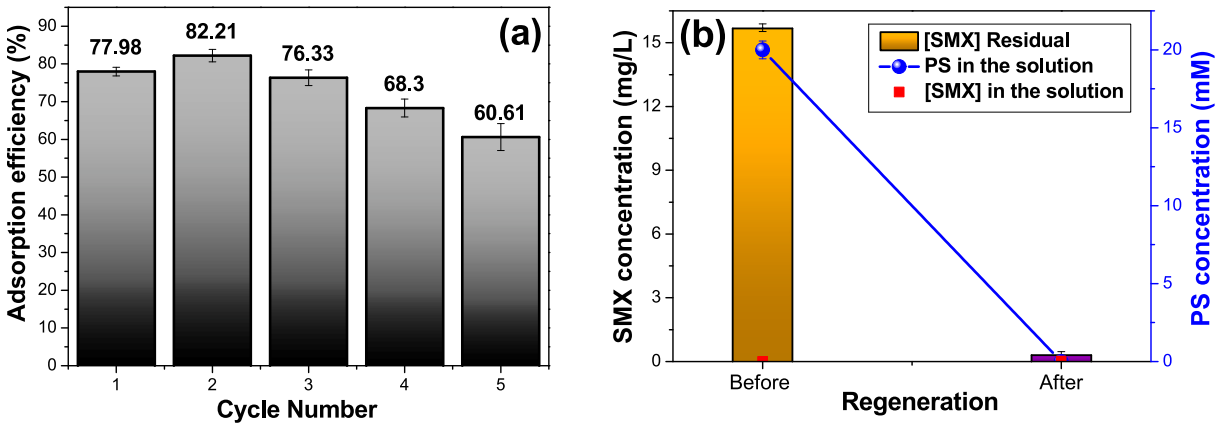

Fig. 5. **(a)** Reusability of biochar for five successive cycles after regeneration, **(b)** Analysis of SMX and PS concentrations during the regeneration process. [SMX] = 5 mg/L, [PS] = 20 mM, Z = 5.5 cm, T = 60 °C.

regeneration, dropping from over 15.67 mg/L to LOD mg/L. This confirms that almost all adsorbed SMX was removed. Based on these findings, it could be concluded that SMX was effectively degraded because it was undetectable in both the biochar and the regeneration solution after regeneration.

3.3. Characterization of adsorbent

The biochar surface morphology after each stage was evaluated using SEM analysis. Fig. 6 displays SEM images of the biochar before and after adsorption and regeneration at a magnification of 200 µm, whereas Figure SM4 shows a magnification of 500 µm. The SEM image of raw biochar (Fig. 6 a) shows a typical morphology of wood-derived material, with an irregular surface and heterogeneous pore sizes and shapes. After adsorption (Fig. 6 b), the biochar surface analysis showed fewer empty pores, as they presumably became filled with SMX molecules, resulting in a possible decrease in the adsorbing surface. Regeneration (Fig. 6 c) resulted in a more regular structure, with both narrow and wide pores, and a smoother surface. This change in morphology is more visible in Fig. 6 d, which shows the biochar after 5 cycles of regeneration. From the image, it is possible to observe a biochar with a more regular and smooth superficial structure and uniformly distributed pores.

The Raman spectra of the biochar after each stage were also assessed and are shown in Fig. 7. Two distinct peaks were identified in all samples: the D-band, which indicates a disordered carbon lattice and aromatics (1357 cm^{-1}), and the G-band, associated with sp^2-bonded carbon (1624 cm^{-1}), which is characterized by a more organized and ordered structure [51]. Almost all of the samples were identical, with only a

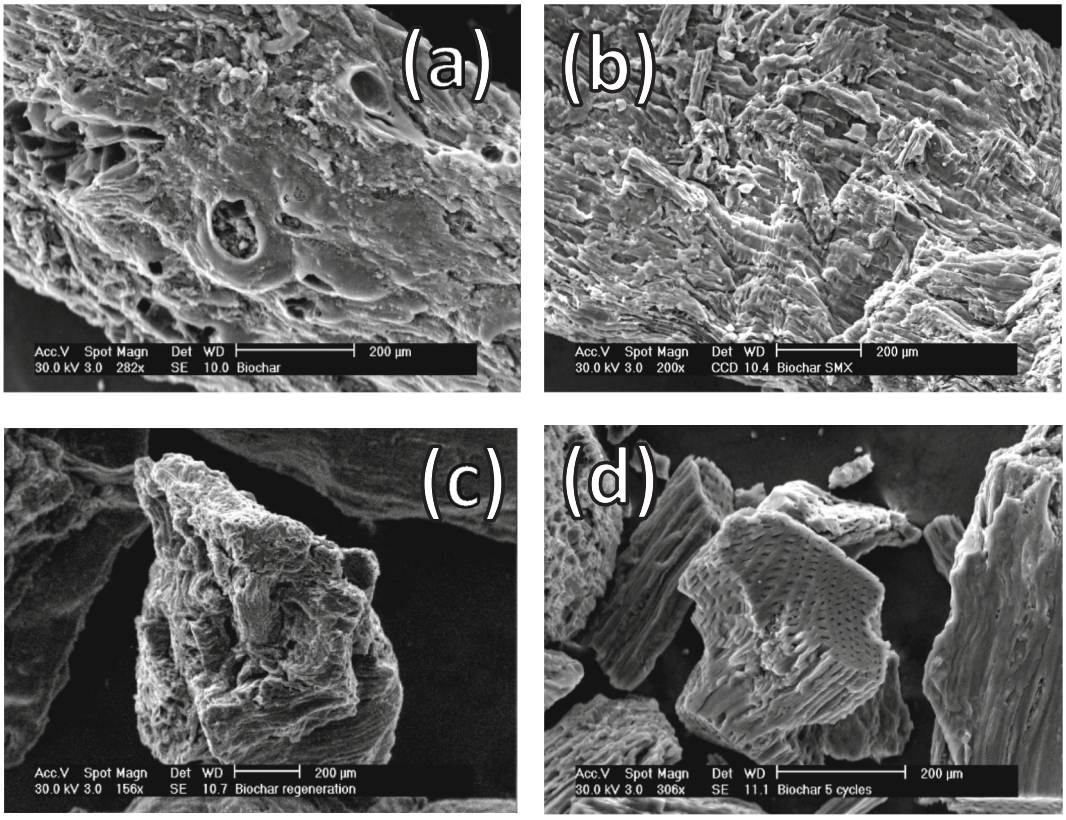

Fig. 6. SEM micrographs of the biochar with a magnification of 200 µm, **(a)** raw, **(b)** after adsorption, **(c)** after regeneration, and **(d)** after 5 cycles.

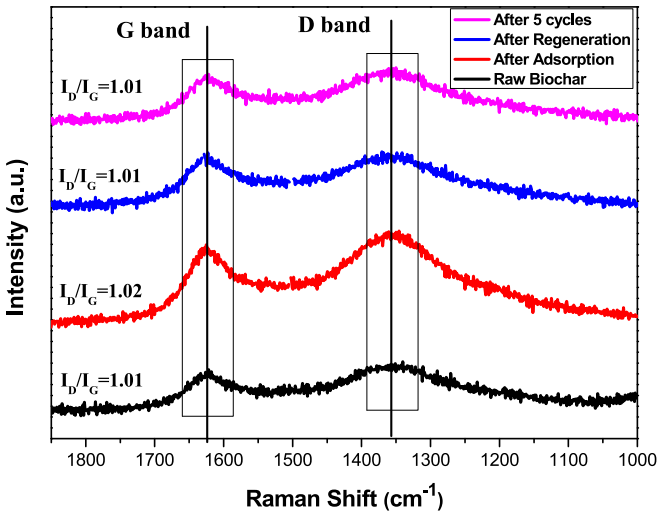

Fig. 7. Raman spectra of the biochar before and after adsorption and regeneration.

change in shape and intensity observed post-adsorption, accompanied by a modification in the D/G ratio, identifying defects in the samples [52]. In fact, a higher D/G ratio indicates increased defects and disorder within the carbon material [53]. The D/G ratio was found to be 1.01 for both the raw and regenerated samples, while, after adsorption, it was 1.02. This alteration in D/G after adsorption results from the SMX interaction with the biochar surface through π-π interactions, wherein the π-electrons of the biochar engage with the π-electrons of the SMX aromatic ring [54]. The Raman analysis also revealed no significant structural changes in the biochar even after five regeneration cycles, suggesting that it maintains its structural integrity and functionality throughout the regeneration process.

Validation of SMX adsorption on biochar is important to confirm its adsorption and removal, which can be done by analyzing the material using XPS before and after SMX adsorption and regeneration [55]. Fig. 8 illustrates the XPS spectra of biochar before and following adsorption and regeneration. The XPS survey spectrum of biochar shown in Fig. 8 (a) and its zoomed-in view in Fig. 8 (b) shows the existence of photoelectronic and Auger (AES) signals in all samples, which include the photoelectronic peaks of C1s and O1s, as well as the associated Auger signals of C KLL and O KLL. These peaks are commonly associated with biochar, which has a structure of aromatic carbon arranged in well-organized layers [56]. After SMX adsorption, the spectrum exhibited a small N1s peak attributable to interactions between carboxyl ($–COO^-$) groups on the biochar surface and amine ($–NH_3^+$) groups from SMX [57]. This peak did not appear either before SMX adsorption or after regeneration, thereby confirming the adsorption of SMX onto the biochar and its subsequent removal post-regeneration, thus aligning with the Raman spectra results. Furthermore, the XPS spectra showed sulfur, with the S2p peak after adsorption and regeneration. A detailed scan of XPS spectra of the S2p region was used to analyze the source of sulfur in both samples before and after regeneration (Fig. 8 c and d). Fig. 8c shows a

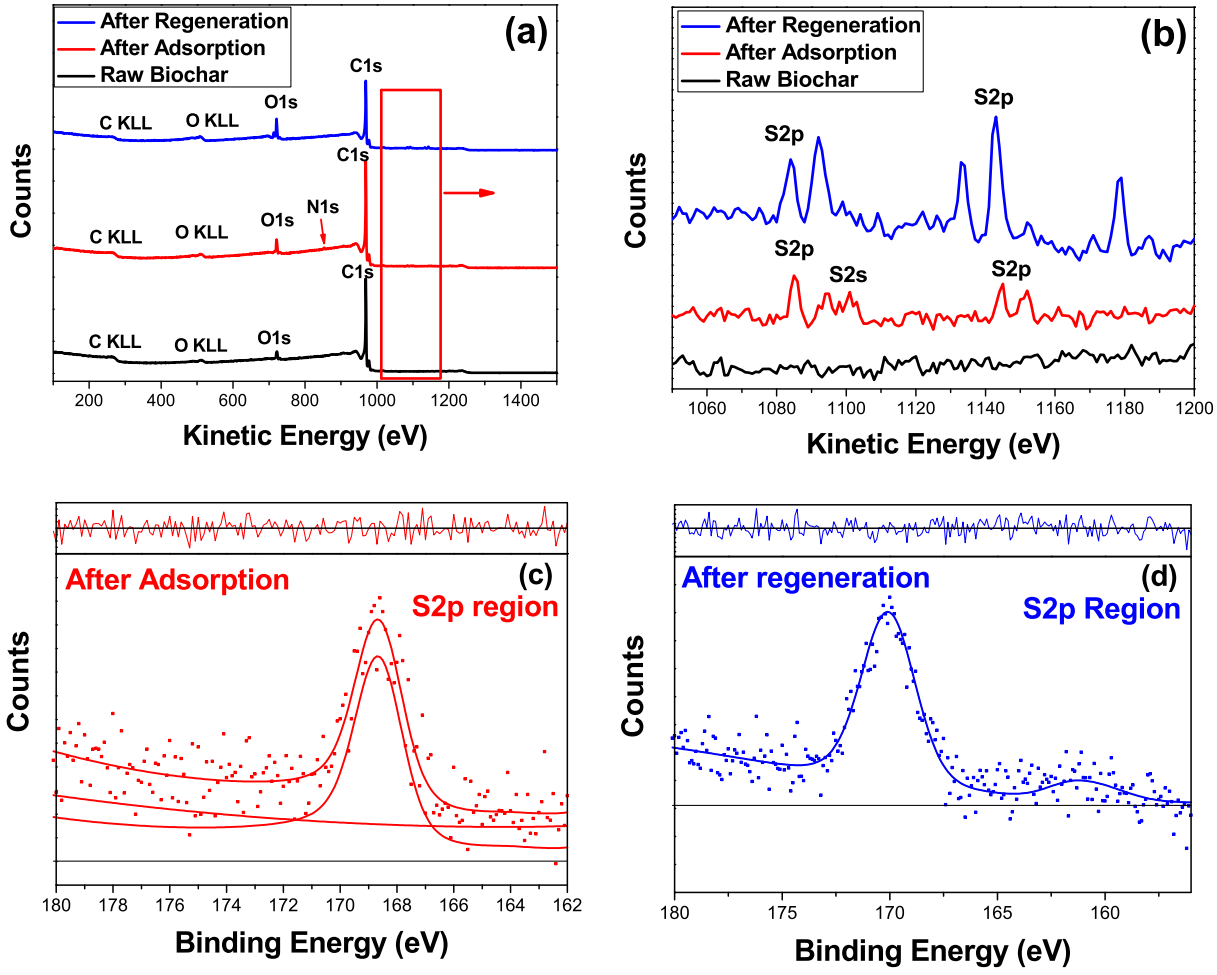

Fig. 8. XPS spectrum of the biochar before and after adsorption and regeneration, **(a)** survey spectrum, **(b)** zoomed-in spectrum, **(c)** XPS spectra of S2p region after adsorption, and **(d)** after regeneration.

distinct peak at approximately 168 eV after adsorption, associated with the sulfur in the sulfonamide group (–SO_2–). Fig. 8 d shows a distinct peak at approximately 170 eV after regeneration (indicating higher binding energy), which is associated with the sulfur of the sulfate radicals ($SO_4^{\bullet-}$) resulting from persulfate activation [58]. XPS spectra of the C1s and O1s regions of the biochar before and after adsorption and regeneration are provided in Figure SM5.

3.4. Validation on real surface and wastewater

The implementation of a biochar fixed bed column on a larger scale necessitates a prior evaluation of its performance using realistic water matrices. The adsorption efficiency may be influenced by inorganic or organic compounds, which could be present in real water samples, such as carbonates, waxes, dyes, silicates, and heavy metals [59]. A non-targeted analysis was employed to screen real samples, as it permits the determination of unknown or unexpected micropollutants [60,61]. The results indicated the presence of pharmaceuticals in both surface water and wastewater samples before treatment, with most contaminants decreasing to below the detection limit after treatment. The compounds detected and subsequently removed by the biochar treatment were atenolol, cetirizine, climbazole, and cotinine (Table 3). In light of these results, the proposed system significantly improved water quality by reducing most of the pollutants detected in both surface water and wastewater, thus suggesting its applicability even in complex matrices.

The turbidity of the real water samples was also monitored during the treatment process. The two surface water samples analyzed had different turbidity levels: one (sample 1, collected from a city river) with high turbidity (T_0 = 22 NTU, Nephelometric Turbidity Unit), and another (sample 2, collected from a dam) with relatively low turbidity (T_0 = 5.68 NTU). Fig. 9 illustrates the significant reduction in turbidity of both water samples after treatment with a biochar fixed-bed column, where the turbidity of the first 500 mL measured ranged from 4.2 to 5.8 NTU (mean: 5 NTU) for sample 1 and 2.0–2.8 NTU (mean: 2.4 NTU) for sample 2. The results demonstrated that the treatment method effectively reduced turbidity in both surface water samples to levels ≤ 5 NTU, which meets the standards for processed food crops [62] and unrestricted vegetable irrigation (<10 NTU) [63]. Additionally, wastewater discharge limits typically target < 10 NTU for environmental safety, according to the Environmental Protection Agency (EPA) [64]. The turbidity of the wastewater sample, which was collected from the outflow of a secondary wastewater treatment unit, was already low (0.75 NTU) before treatment and improved slightly to 0.7 NTU after treatment.

3.5. Design and techno-economic evaluation for scaling up the system

An engineering design for an adsorption removal unit using biochar was proposed based on prior experimental results. Scaling up the adsorption system parameters was done by using a scaling factor [65], which can be used to estimate parameters from small to larger-scale systems. The scaling factor (100) was determined using a target flow rate ($Q_{scaled\text{-}up}$ = 1 L/min). Starting with scaling up the column volume, the previous experimental volume was $V_{original} \approx 83.5$ mL, which, when multiplied by the scaling factor, yields $V_{scaled\text{-}up}$ = 8.35 L. The diameter (D = 11.6 cm) and length (L = 79 cm) of the scaled-up column were determined by calculating them based on the cube root of the scaling factor (4.64), as the column is scaled up geometrically [66]. The biochar mass is proportional to the bed volume and was calculated using the scaling factor, which was found to be 2.3 kg. Table SM5 summarizes the parameters of the original setup versus the scaled-up one.

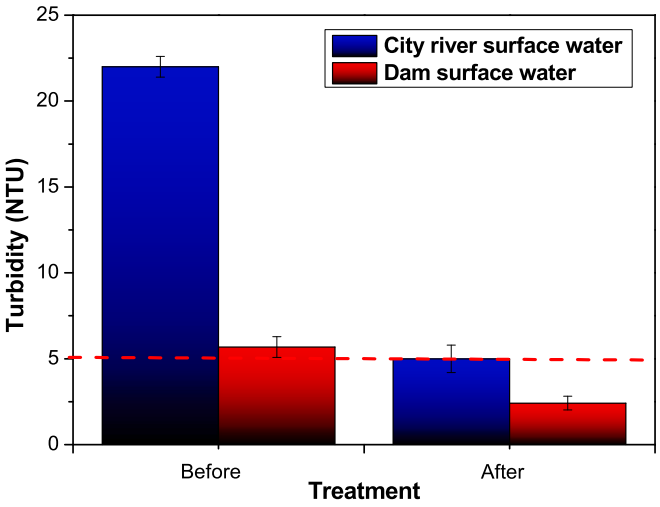

Fig. 9. Turbidity of surface water before and after the treatment.

In order to provide a viable and well-developed approach to treating such complex water, an engineering perspective was applied to outline the general column shape, dimensions, and quantity while emphasizing the optimal installation of the treatment units and clarifying the water flow within the system. To effectively remove pollutants from wastewater and surface water and minimize treatment time, a dual-function treatment system consisting of two parallel columns that alternately treat and regenerate was proposed to ensure continuous operation. The treated water is discharged into a tank to be reused for other purposes, such as agricultural irrigation, where the regeneration solution is stored in another tank to dispose of degradation byproducts generated from the regeneration method safely. Fig. 10 depicts a schematic diagram of the proposed treatment unit, detailing the operational process for treating polluted effluent as well as column regeneration.

The economic feasibility evaluation is essential for evaluating the financial feasibility of the proposed treatment system [67–69]; For that, the proposed system was evaluated under previously established conditions, maintaining a flow rate of 1 L/min as a scale-neutral parameter to facilitate the design of larger-scale systems. The breakthrough time was estimated to be 130 h for each column, as previously estimated. The total cost of implementing the proposed system was estimated to be around €260, with the cost for each column (79 cm in length and 11.6 cm internal diameter, made of 304 stainless steel with a wall thickness of 3 mm) being approximately €21 based on the average price in Europe, where the remaining costs covered other components like pipes, valves, pumps, and tanks. The cost of the adsorbent material for two columns is €26.31, while the regeneration process reduces this cost through reuse. The cost of a regeneration solution (PS) is €0.24/L with a concentration of 20 mM, based on the price for PS (€49.60/kg), which can produce 210 L of solution. Operating expenditure was approximated at the average of €0.31/m^3 [70], including operations, maintenance, heating energy, and pumping. Costs related to maintenance, workers, and land were not

Table 3
Pollutants detected and removed from surface water and wastewater.

Contaminant	Matrix	Detected concentration (µg/L)	Concentration after treatment (µg/L)	LOD (µg/L)
Atenolol	Surface Water	9.04 ± 0.081	<LOD	2.15
	Wastewater	6.89 ± 0.016	<LOD	
Cetirizine	Surface Water	20.86 ± 0.136	<LOD	5.6
	Wastewater	32.16 ± 0.156	<LOD	
Climbazole	Surface Water	4.13 ± 0.072	<LOD	1.7
	Wastewater	1.71 ± 0.055	<LOD	
Cotinine	Surface Water	15.31 ± 0.164	<LOD	2.8
	Wastewater	<LOD	<LOD	

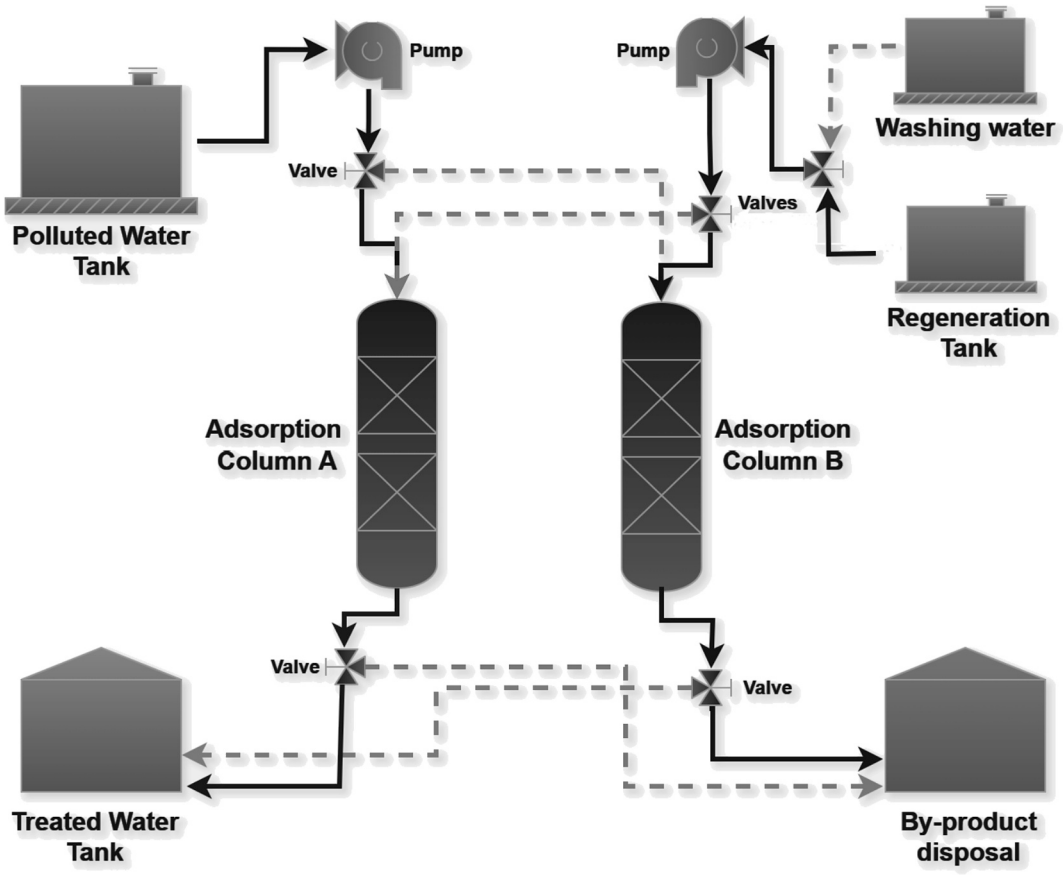

Fig. 10. Schematic diagram of the proposed dual-column adsorption-based water treatment system.

included in calculations as they are not a governing criterion for the treatment system [71]. The costs are summarized in Table 4, and based on these values, the treatment cost was estimated to be €0.89/m^3. The cost of this treatment method was found to be acceptable when compared to other methods, where treatment costs usually range between 0.30 and €2.94/m^3 [72,73], and in certain cases can exceed €5.00/m^3, such as reverse osmosis treatment [74].

Breakeven analysis was used to trade off the cost of effluent treatment between the proposed in-plant treatment system and off-plant treatment works [75,76], considering an average off-plant treatment cost of about €2.65/m^3 [77,78]. Fig. 11 (a) displays the break-even analysis comparing the suggested in-plant to off-plant treatment. The system's construction cost (€423.96) was regarded as a fixed cost, while its treatment cost (€0.89/m^3) was regarded as a variable cost. The amount of wastewater at which the costs of in-plant treatment and off-plant treatment are equal is known as the break-even quantity, and it was estimated to be 240 m^3.

Payback analysis was used to assess the system's minimum operational lifespan required to repay the capital expenditures by comparing the cost of the in-plant treatment with the off-plant water treatment price. The payback period was estimated by adjusting treatment volume (Q) based on months of treatment (30 m^3 per month) and profit, as illustrated in Fig. 11 (b). The payback period has been predicted to be 8 months, which indicates fast and efficient cost recovery and quick reinvestment compared to other treatment methods, such as photocatalysis [71], making the process financially viable and economically feasible.

Table 4
Economic evaluation for the proposed dual-column adsorption-based water treatment system.

Parameter	Value
Flow rate	1 L/min
Estimated working days per year	250 days/year
Treated wastewater (m^3/day)	1.44 m^3/day
Breakthrough time	130 h
Column volume	8.35 L
Column number	2
Column system (stainless steel)	€21
System implementation cost	€260
Biochar cost	€5.72/kg
Adsorbent amount per column	2.3 Kg
Estimated operating costs	€0.31/m^3
Regeneration solution cost	€0.24/L
Estimated treatment cost	€0.89/m^3

4. Conclusions

This study investigated the feasibility of using biochar as a water treatment method in a downflow fixed-bed adsorption system for removing contaminants from surface water and wastewater. The process parameters, such as flow rate and bed length, were optimized by conducting rapid small-scale column tests to remove the commonly used antibiotic SMX. This process, which used a column with a 12.5 cm adsorbent bed depth, demonstrated that it could continue functioning for up to 130 h, achieving an 80 % saturation rate after treating 33 L of 5 mg/L SMX. Adsorption kinetics and breakthrough curves were analyzed using kinetic models such as Adams-Bohart, Thomas, Clark, and Yoon-Nelson. The Clark model demonstrated the highest degree of fit to the data, as it combines the Freundlich isotherm and a mass transfer theory, implying that it can be used to predict the breakthrough curve. The system's reusability was also studied using a novel continuous regeneration approach and by monitoring changes in the adsorbent through characterization techniques, demonstrating reusability with larger pores

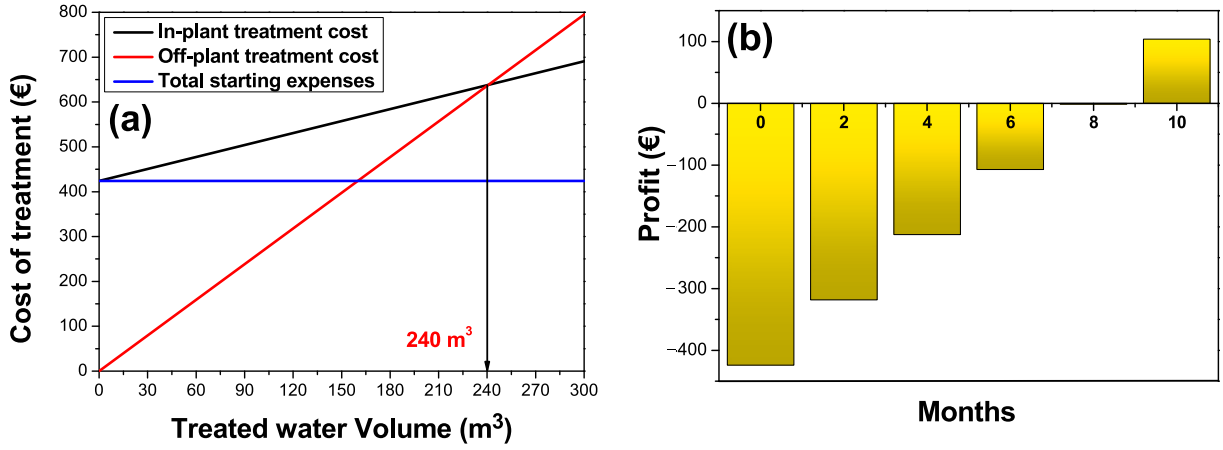

Fig. 11. **(a)** Break-even analysis, **(b)** Payback period analysis of the proposed water treatment system.

and more effective contaminant removal compared to the literature. The applicability of this system was further confirmed by experiments on real contaminated samples by following contaminants and turbidity, which showed a significant reduction in both. Finally, a dual-column adsorption-based water treatment system was proposed for large-scale applications, and a techno-economic study was conducted to evaluate its feasibility, where it was demonstrated that the unit cost of this process could be estimated to be €0.89/m^3, which can be considered commercially and economically feasible. The study found that biochar has the potential to be an economically effective water treatment solution that can be scaled up for industrial applications. To increase treated water quality, future research should focus on improving this approach and enhancing treatment efficiency by combining it with other efficient treatment methods.

CRediT authorship contribution statement

Oussama Baaloudj: Conceptualization, Writing – original draft, Writing – review & editing, Methodology, Investigation. **Fausto Langerame:** Investigation. **Rocco Iunnissi:** Investigation. **Gianluigi Buttiglieri:** Investigation. **Daniele Del Buono:** Investigation. **Samia Khadhar:** Investigation. **Laura Scrano:** Investigation. **Vincenzo Trotta:** Writing – review & editing. **Monica Brienza:** Conceptualization, Funding acquisition, Writing – review & editing, Methodology, Supervision.

Declaration of competing interest

The authors declare that they have no known competing financial interests or personal relationships that could have appeared to influence the work reported in this paper.

Acknowledgement

This research has been partially funded by MUR under the umbrella of the PRIMA — Partnership for Research & Innovation in the Mediterranean Area — through the SAFE project (ID 1826), and partially through the NeWater under the umbrella of the WATER4ALL Partnership. It has also received support from the Consolidated Research Group ICRA-ENV-2021 SGR 01282 and ICRA-TECH-2021 SGR 01283, funded by the Economy and Knowledge Department of the Catalan Government, and from AquaLoops4Med (Grant Agreement n° 101161349) under the European Union's I3 Instrument initiative. The authors would like to thank Alessandro Laurita for performing the SEM analysis and Prof. Angela De Bonis for the Raman analysis.

Appendix A. Supplementary data

Supplementary data to this article can be found online at https://doi.org/10.1016/j.seppur.2025.134347.

Data availability

Data will be made available on request.

References

[1] N. Talreja, C. Hegde, E.M. Kumar, M. Chavali, Emerging Environmental Contaminants: sources, Consequences and Future Challenges (2025), https://doi.org/10.1002/9781394159390.ch5.
[2] N. Zaidi, M.A. Mir, S.K. Chang, N. Abdelli, S.M. Hasnain, M.A. Ali Khan, K. Andrews, Pharmaceuticals and personal care products as emerging contaminants: environmental fate, detection, and mitigation strategies, Int. J. Environ. Anal. Chem. (2025), https://doi.org/10.1080/03067319.2025.2484456.
[3] L.O. Omuferen, B. Maseko, J.O. Olowoyo, Occurrence of antibiotics in wastewater from hospital and convectional wastewater treatment plants and their impact on the effluent receiving rivers: current knowledge between 2010 and 2019, Environ. Monit. Assess. 194 (2022), https://doi.org/10.1007/s10661-022-09846-4.
[4] S. Akhter, M.A. Bhat, S. Ahmed, W.A. Siddiqui, Antibiotic residue contamination in the aquatic environment, sources and associated potential health risks, Environ. Geochem. Health 46 (2024), https://doi.org/10.1007/s10653-024-02146-5.
[5] B.S. Diogo, S. Rodrigues, O. Golovko, S.C. Antunes, From bacteria to fish: ecotoxicological insights into sulfamethoxazole and trimethoprim, Environ. Sci. Pollut. Res. 31 (2024) 52233–52252, https://doi.org/10.1007/s11356-024-34659-y.
[6] M. Qu, J. Xu, Y. Yang, R. Li, T. Li, S. Chen, Y. Di, Assessment of sulfamethoxazole toxicity to marine mussels (Mytilus galloprovincialis): Combine p38-MAPK signaling pathway modulation with histopathological alterations, Ecotoxicol. Environ. Saf. 249 (2023), https://doi.org/10.1016/j.ecoenv.2022.114365.
[7] J. Farrell, D.J. Naisbitt, N.S. Drummond, J.P.H. Depta, F.J. Vilar, M. Pirmohamed, B.K. Park, Characterization of sulfamethoxazole and sulfamethoxazole metabolite-specific T-cell responses in animals and humans, J. Pharmacol. Exp. Ther. 306 (2003) 229–237, https://doi.org/10.1124/jpet.103.050112.
[8] X. Peng, X. Zhang, S. Zhang, Z. Li, H. Zhang, L. Zhang, Z. Wu, B. Liu, Revealing the response characteristics of periphyton biomass and community structure to sulfamethoxazole exposure in aquaculture water: the perspective of microbial network relationships, Environ. Pollut. 344 (2024), https://doi.org/10.1016/j.envpol.2024.123301.
[9] M. Nazir, M.I. Aziz, I. Ali, M.A. Basit, Revealing antimicrobial and contrasting photocatalytic behavior of metal chalcogenide deposited P25-TiO2 nanoparticles, Photonics Nanostructures - Fundam. Appl. 36 (2019) 100721, https://doi.org/10.1016/j.photonics.2019.100721.
[10] E. Mousset, W.H. Loh, W.S. Lim, L. Jarry, Z. Wang, O. Lefebvre, Cost comparison of advanced oxidation processes for wastewater treatment using accumulated oxygen-equivalent criteria, Water Res. 200 (2021), https://doi.org/10.1016/j.watres.2021.117234.
[11] R.S. Dhamorikar, V.G. Lade, P.V. Kewalramani, A.B. Bindwal, Review on integrated advanced oxidation processes for water and wastewater treatment, J. Ind. Eng. Chem. 138 (2024) 104–122, https://doi.org/10.1016/j.jiec.2024.04.037.
[12] R. Binjhade, R. Mondal, S. Mondal, Continuous photocatalytic reactor: critical review on the design and performance, J. Environ. Chem. Eng. 10 (2022), https://doi.org/10.1016/j.jece.2022.107746.

[13] M. Bizi, Sulfamethoxazole Removal from Drinking Water by Activated Carbon: Kinetics and Diffusion Process, Molecules 25 (2020), https://doi.org/10.3390/molecules25204656.
[14] B.M. Rizkallah, M.M. Galal, M.E. Matta, Characteristics of Tetracycline Adsorption on Commercial Biochar from Synthetic and Real Wastewater in batch and Continuous Operations: Study of Removal Mechanisms, Isotherms, Kinetics, Thermodynamics, and Desorption, Sustain 15 (2023), https://doi.org/10.3390/su15108249.
[15] M. Mujtaba, L. Fernandes Fraceto, M. Fazeli, S. Mukherjee, S.M. Savassa, G. Araujo de Medeiros, A. do Espírito Santo Pereira, S.D. Mancini, J. Lipponen, F. Vilaplana, Lignocellulosic biomass from agricultural waste to the circular economy: a review with focus on biofuels, biocomposites and bioplastics, J. Clean. Prod. 402 (2023), https://doi.org/10.1016/j.jclepro.2023.136815.
[16] Y.E. Lee, D.C. Shin, Y. Jeong, I.T. Kim, Y.S. Yoo, Pyrolytic valorization of water treatment residuals containing powdered activated carbon as multifunctional adsorbents, Chemosphere 252 (2020), https://doi.org/10.1016/j.chemosphere.2020.126641.
[17] O. Samuel Olugbenga, P. Goodness Adeleye, S. Blessing Oladipupo, A. Timothy Adeleye, K. Igenepo John, Biomass-derived biochar in wastewater treatment- a circular economy approach, Waste Manag, Bull. Georgian Acad. Sci. 1 (2024) 1–14, https://doi.org/10.1016/j.wmb.2023.07.007.
[18] V.K.H. Bui, T.P. Nguyen, T.C.P. Tran, T.T.N. Nguyen, T.N. Duong, V.T. Nguyen, C. Liu, D.D. Nguyen, X.C. Nguyen, Biochar-based fixed filter columns for water treatment: a comprehensive review, Sci. Total Environ. 954 (2024), https://doi.org/10.1016/j.scitotenv.2024.176199.
[19] S. Kalsoom, R. Khan, M. Ullah, A. Adil, K.A. Waheed, H.A. Khan, H.F. Ghramh, Y. M. Alharby, S.A. Alzahrani, N.M. Alghamdi, F. Alabdallah, Rahim, Adsorption of Pesticides using Wood-Derived Biochar and Granular Activated Carbon in a Fixed-Bed Column System, Water (switzerland). 14 (2022), https://doi.org/10.3390/w14192937.
[20] X. Xu, W. Feng, L. Guo, X. Huang, B. Shi, Controlled synthesis of distiller's grains biochar for turbidity removal in Baijiu, Sci. Total Environ. 867 (2023), https://doi.org/10.1016/j.scitotenv.2022.161382.
[21] A. Sochacki, M. Lebrun, B. Minofar, M. Pohořelý, M. Vithanage, A.K. Sarmah, B. Böserle Hudcová, S. Buchtelík, L. Trakal, Adsorption of common greywater pollutants and nutrients by various biochars as potential amendments for nature-based systems: Laboratory tests and molecular dynamics, Environ. Pollut. 343 (2024), https://doi.org/10.1016/j.envpol.2023.123203.
[22] S. Minaei, K. Zoroufchi Benis, K.N. McPhedran, J. Soltan, Adsorption of sulfamethoxazole and lincomycin from single and binary aqueous systems using acid-modified biochar from activated sludge biomass, J. Environ. Manage. 358 (2024), https://doi.org/10.1016/j.jenvman.2024.120742.
[23] O. Baaloudj, S. Chiron, A.R. Zizzamia, V. Trotta, D. Del Buono, D. Puglia, M. Rallini, M. Brienza, Efficient biochar regeneration for a circular economy: Removing emerging contaminants for sustainable water treatment, Colloids Surfaces A Physicochem. Eng. Asp. 705 (2025) 135730, https://doi.org/10.1016/j.colsurfa.2024.135730.
[24] J. Huang, A.R. Zimmerman, H. Chen, Y. Wan, Y. Zheng, Y. Yang, Y. Zhang, B. Gao, Fixed bed column performance of Al-modified biochar for the removal of sulfamethoxazole and sulfapyridine antibiotics from wastewater, Chemosphere 305 (2022), https://doi.org/10.1016/j.chemosphere.2022.135475.
[25] V.K. Gupta, I. Suhas, S. Tyagi, R. Agarwal, M. Singh, A. Chaudhary, S. Harit, Kushwaha, Column operation studies for the removal of dyes and phenols using a low cost adsorbent, Glob. J. Environ. Sci. Manag. 2 (2016) 1–10, https://doi.org/10.7508/gjesm.2016.01.001.
[26] C. Li, N. de Melo Costa, R.F.P. Serge, S. Nogueira, V.G. Chiron, Peroxydisulfate activation by CuO pellets in a fixed-bed column, operating mode and assessments for antibiotics degradation and urban wastewater disinfection, Environ. Sci. Pollut. Res. 29 (2022) 71709–71720, https://doi.org/10.1007/s11356-022-20847-1.
[27] H. Patel, Fixed-bed column adsorption study: a comprehensive review, Appl Water Sci 9 (2019), https://doi.org/10.1007/s13201-019-0927-7.
[28] H. Patel, Comparison of batch and fixed bed column adsorption: a critical review, Int. J. Environ. Sci. Technol. (2021), https://doi.org/10.1007/s13762-021-03492-y.
[29] M.M.R. Khan, M.W. Rahman, M.S.I. Mozumder, K. Ferdous, H.R. Ong, K.M. Chan, D.M.R. Prasad, Performance of a submerged adsorption column compared with conventional fixed-bed adsorption, Desalin. Water Treat. 57 (2016) 9705–9717, https://doi.org/10.1080/19443994.2015.1030779.
[30] K.M. Mena aguilat, Y. A, ano, M. Machida, Ammonium Persulfate Oxidized Activated Carbon Fibers: Analysis of Their Oxidation Debris Quantity and Their Use for Aqueous Pb(II) Batch and Column Experiments, J. Fiber Sci. Technol. 73 (2017) 150–157. Doi: 10.2115/fiberst.2017-0021.
[31] M.M. Rahman, M. Maniruzzaman, M.S. Yeasmin, M.A. Gafur, M.A.A. Shaikh, M. A. Alam, M.J. Uddin, M. Hasan, M. Al Bashera, T.A. Chowdhury, B. Maitra, M. R. Naim, G.M.M. Rana, B.K. Saha, M.S. Quddus, Adsorptive abatement of Pb2+ and crystal violet using chitosan-modified coal nanocomposites: a down flow column study, Groundw. Sustain. Dev. 23 (2023), https://doi.org/10.1016/j.gsd.2023.101028.
[32] N. Delgado, D. Marino, A. Capparelli, J.C. Casas-Zapata, A. Navarro, Pharmaceutical compound removal using down-flow fixed bed filters with powder activated carbon: a novel configuration, J. Environ. Chem. Eng. 10 (2022), https://doi.org/10.1016/j.jece.2022.107706.
[33] F. Zietzschmann, J. Müller, A. Sperlich, A.S. Ruhl, F. Meinel, J. Altmann, M. Jekel, Rapid small-scale column testing of granular activated carbon for organic micro-pollutant removal in treated domestic wastewater, Water Sci. Technol. 70 (2014) 1271–1278, https://doi.org/10.2166/wst.2014.357.
[34] F. Feizi, A.K. Sarmah, R. Rangsivek, Adsorption of pharmaceuticals in a fixed-bed column using tyre-based activated carbon: Experimental investigations and numerical modelling, J. Hazard. Mater. 417 (2021), https://doi.org/10.1016/j.jhazmat.2021.126010.
[35] Đ. Tadić, R. Manasfi, M. Bertrand, A. Sauvêtre, S. Chiron, Use of Passive and Grab Sampling and High-Resolution Mass Spectrometry for Non-Targeted Analysis of Emerging Contaminants and their Semi-Quantification in Water, Molecules 27 (2022), https://doi.org/10.3390/molecules27103167.
[36] J. Matolia, S.P. Shukla, S. Kumar, K. Kumar, A.R. Singh, Physical entrapment of chitosan in fixed-down-flow column bed enhances triclosan removal from water, Water Sci. Technol. 80 (2019) 1374–1383, https://doi.org/10.2166/wst.2019.386.
[37] H.C.B. Man, C.O. Akinbile, C.X. Jun, Coconut husk adsorbent for the removal of methylene blue dye from wastewater, BioResources 10 (2015) 2859–2872, https://doi.org/10.15376/biores.10.2.2859-2872.
[38] V. Parimelazhagan, G. Jeppu, N. Rampal, Continuous fixed-bed column studies on congo red dye adsorption-desorption using free and immobilized nelumbo nucifera leaf adsorbent, Polymers (basel). 14 (2022), https://doi.org/10.3390/polym14010054.
[39] H. Salmani, A comparative study of copper (ii) removal on iron oxide, aluminum oxide and activated carbon by continuous down flow method, J. Toxicol. Environ. Heal. Sci. 5 (2013) 150–155, https://doi.org/10.5897/jtehs2013.0275.
[40] C. Djelloul, O. Hamdaoui, Dynamic adsorption of methylene blue by melon peel in fixed-bed columns, Desalin. Water Treat. 56 (2015) 2966–2975, https://doi.org/10.1080/19443994.2014.963158.
[41] M. Oteng-Peprah, P.A. Obeng, M.A. Acheampong, M.A. Anang, Fixed-bed column sorption kinetic rates on the removal of both biochemical oxygen demand (BOD5) and chemical oxygen demand (COD) in domestic greywater by using palm kernel activated carbon, Water Pract. Technol. 18 (2023) 1628–1638, https://doi.org/10.2166/wpt.2023.097.
[42] A.A. Abin-Bazaine, M.A. Olmos-Marquez, A. Campos-Trujillo, A Fixed-Bed Column Sorption: Breakthrough Curves Modeling, Sorption - New Perspect, Appl. [working Title]. (2024), https://doi.org/10.5772/intechopen.1004446.
[43] J. Deng, Y. Fang, C. Hou, Y. Zhang, M. Li, J. Han, W.X. Du, C. Tang, X. Hu, Ultrasonic assisted activation of persulfate for the treatment of spent porous biochar: Degradation of adsorbed PFOA and adsorbent regeneration, J. Environ. Chem. Eng. 11 (2023), https://doi.org/10.1016/j.jece.2023.111146.
[44] S. Ahmadi, C.A. Igwegbe, S. Rahdar, The application of thermally activated persulfate for degradation of Acid Blue 92 in aqueous solution, Int. J. Ind. Chem. 10 (2019) 249–260, https://doi.org/10.1007/s40090-019-0188-1.
[45] X.R. Jing, Y.Y. Wang, W.J. Liu, Y.K. Wang, H. Jiang, Enhanced adsorption performance of tetracycline in aqueous solutions by methanol-modified biochar, Chem. Eng. J. 248 (2014) 168–174, https://doi.org/10.1016/j.cej.2014.03.006.
[46] C.A. Igwegbe, C.J. Umembamalu, E.U. Osuagwu, S.N. Oba, L.N. Emembolu, Studies on Adsorption Characteristics of Corn Cobs Activated Carbon for the Removal of Oil and Grease from Oil Refinery Desalter Effluent in a Downflow Fixed Bed Adsorption Equipment, Eur. J. Sustain. Dev. Res. 5 (2020) em0145, https://doi.org/10.29333/ejosdr/9285.
[47] Z. Xu, J.G. Cai, B.C. Pan, Mathematically modeling fixed-bed adsorption in aqueous systems, J. Zhejiang Univ. Sci. a. 14 (2013) 155–176, https://doi.org/10.1631/jzus.A1300029.
[48] N. Al-Mahbashi, S.R.M. Kutty, A.H. Jagaba, A. Al-Nini, M. Ali, A.A.H. Saeed, A.A. S. Ghaleb, U. Rathnayake, Column Study for Adsorption of copper and Cadmium using Activated Carbon Derived from Sewage Sludge, Adv. Civ. Eng. 2022 (2022), https://doi.org/10.1155/2022/3590462.
[49] T. Alsawy, E. Rashad, M. El-Qelish, R.H. Mohammed, A comprehensive review on the chemical regeneration of biochar adsorbent for sustainable wastewater treatment, npj Clean Water 5 (2022), https://doi.org/10.1038/s41545-022-00172-3.
[50] C. Liang, C.F. Huang, N. Mohanty, R.M. Kurakalva, A rapid spectrophotometric determination of persulfate anion in ISCO, Chemosphere 73 (2008) 1540–1543, https://doi.org/10.1016/j.chemosphere.2008.08.043.
[51] E. Grilla, J. Vakros, I. Konstantinou, I.D. Manariotis, D. Mantzavinos, Activation of persulfate by biochar from spent malt rootlets for the degradation of trimethoprim in the presence of inorganic ions, J. Chem. Technol. Biotechnol. 95 (2020) 2348–2358, https://doi.org/10.1002/jctb.6513.
[52] Q. Zhao, Z. Xu, Z. Yu, Straw-derived biochar as the potential adsorbent for U(VI) and Th(IV) removal in aqueous solutions, Biomass Convers. Biorefinery. 13 (2023) 15707–15718, https://doi.org/10.1007/s13399-021-01810-5.
[53] T. Palaniselvam, H.B. Aiyappa, S. Kurungot, An efficient oxygen reduction electrocatalyst from graphene by simultaneously generating pores and nitrogen doped active sites, J. Mater. Chem. 22 (2012) 23799–23805, https://doi.org/10.1039/c2jm35128e.
[54] R. Zhang, X. Zheng, B. Chen, J. Ma, X. Niu, D. Zhang, Z. Lin, M. Fu, S. Zhou, Enhanced adsorption of sulfamethoxazole from aqueous solution by Fe-impregnated graphited biochar, J. Clean. Prod. 256 (2020), https://doi.org/10.1016/j.jclepro.2020.120662.
[55] P. Sarker, X. Lei, K. Taylor, W. Holmes, H. Yan, D. Cao, M.E. Zappi, D.D. Gang, Evaluation of the adsorption of sulfamethoxazole (SMX) within aqueous influents onto customized ordered mesoporous carbon (OMC) adsorbents: Performance and elucidation of key adsorption mechanisms, Chem. Eng. J. 454 (2023), https://doi.org/10.1016/j.cej.2022.140082.
[56] S. Ekman, G.S. dos Reis, E. Laisné, J. Thivet, A. Grimm, E.C. Lima, M. Naushad, G. L. Dotto, Synthesis, Characterization, and Adsorption Properties of Nitrogen-Doped Nanoporous Biochar: Efficient Removal of Reactive Orange 16 Dye and Colorful Effluents, Nanomaterials 13 (2023), https://doi.org/10.3390/nano13142045.

[57] A.A. Kadam, B. Sharma, G.D. Saratale, R.G. Saratale, G.S. Ghodake, B.M. Mistry, S. K. Shinde, S.C. Jee, J.S. Sung, Super-magnetization of pectin from orange-peel biomass for sulfamethoxazole adsorption, Cellul. 27 (2020) 3301–3318, https://doi.org/10.1007/s10570-020-02988-z.
[58] X. Huang, Q. Hu, L. Gao, Q. Hao, P. Wang, D. Qin, Adsorption characteristics of metal-organic framework MIL-101(Cr) towards sulfamethoxazole and its persulfate oxidation regeneration, RSC Adv. 8 (2018) 27623–27630, https://doi.org/10.1039/c8ra04789h.
[59] T. Taweekarn, W. Wongniramaikul, W. Sriprom, W. Limsakul, A. Choodum, Continuous-Flow System for Methylene Blue Removal using a Green and Cost-Effective Starch Single-Rod Column, Polymers (basel). 15 (2023), https://doi.org/10.3390/polym15193989.
[60] G. Nürenberg, U. Kunkel, A. Wick, P. Falås, A. Joss, T.A. Ternes, Nontarget analysis: a new tool for the evaluation of wastewater processes, Water Res. 163 (2019), https://doi.org/10.1016/j.watres.2019.07.009.
[61] J. Gwak, J. Lee, J. Cha, M. Kim, J. Hur, J. Cho, M.S. Kim, K.S. Jang, J.P. Giesy, S. Hong, J.S. Khim, Molecular Characterization of Estrogen Receptor Agonists during Sewage Treatment Processes using Effect-Directed Analysis combined with High-Resolution Full-Scan Screening, Environ. Sci. Technol. 56 (2022) 13085–13095, https://doi.org/10.1021/acs.est.2c03428.
[62] P. Jin, X. Jin, X.C. Wang, X. Shi, An analysis of the chemical safety of secondary effluent for reuse purposes and the requirement for advanced treatment, Chemosphere 91 (2013) 558–562, https://doi.org/10.1016/j.chemosphere.2013.01.004.
[63] H. Jeong, H. Kim, T. Jang, Irrigation water quality standards for indirect wastewater reuse in agriculture: a contribution toward sustainablewastewater reuse in South korea, Water (switzerland). 8 (2016), https://doi.org/10.3390/w8040169.
[64] S. Kali, M. Khan, M.S. Ghaffar, S. Rasheed, A. Waseem, M.M. Iqbal, M. Bilal khan Niazi, M.I. Zafar, Occurrence, influencing factors, toxicity, regulations, and abatement approaches for disinfection by-products in chlorinated drinking water: a comprehensive review, Environ. Pollut. 281 (2021), https://doi.org/10.1016/j.envpol.2021.116950.
[65] O. Callery, M.G. Healy, F. Rognard, L. Barthelemy, R.B. Brennan, Evaluating the long-term performance of low-cost adsorbents using small-scale adsorption column experiments, Water Res. 101 (2016) 429–440, https://doi.org/10.1016/j.watres.2016.05.093.
[66] D. Juela, M. Vera, C. Cruzat, A. Astudillo, E. Vanegas, A new approach for scaling up fixed-bed adsorption columns for aqueous systems: a case of antibiotic removal on natural adsorbent, Process Saf. Environ. Prot. 159 (2022) 953–963, https://doi.org/10.1016/j.psep.2022.01.046.
[67] A. Naboulsi, T. Bouzid, A. Grich, A. Regti, M. El Himri, M. El Haddad, Understanding the column and batch adsorption mechanism of pesticide 2,4,5-T utilizing alginate-biomass hydrogel capsule: a computational and economic investigation, Int. J. Biol. Macromol. 275 (2024), https://doi.org/10.1016/j.ijbiomac.2024.133762.
[68] İ. Utku, R. Kaya, T. Türken, İ. Koyuncu, Cost analysis and selection of advanced water treatment methods for organic matter removal, Desalin. Water Treat. 211 (2021) 432–438, https://doi.org/10.5004/dwt.2021.26676.
[69] D. Frascari, A.E. Molina Bacca, T. Wardenaar, E. Oertlé, D. Pinelli, Continuous flow adsorption of phenolic compounds from olive mill wastewater with resin XAD16N: life cycle assessment, cost–benefit analysis and process optimization, J. Chem. Technol. Biotechnol. 94 (2019) 1968–1981, https://doi.org/10.1002/jctb.5980.
[70] E.M. Pajares, L.G. Valero, I.M.R. Sánchez, Cost of urban wastewater treatment and ecotaxes: evidence from municipalities in southern Europe, Water (switzerland). 11 (2019), https://doi.org/10.3390/w11030423.
[71] O. Baaloudj, A.K. Badawi, H. Kenfoud, Y. Benrighi, R. Hassan, N. Nasrallah, A. A. Assadi, Techno-economic studies for a pilot-scale Bi12TiO20 based photocatalytic system for pharmaceutical wastewater treatment: from laboratory studies to commercial-scale applications, J. Water Process Eng. 48 (2022) 102847, https://doi.org/10.1016/j.jwpe.2022.102847.
[72] V. Fabregat, J.M. Pagán, Technical–Economic Feasibility of a New Method of Adsorbent Materials and Advanced Oxidation Techniques to Remove Emerging Pollutants in Treated Wastewater, Water (switzerland). 16 (2024), https://doi.org/10.3390/w16060814.
[73] Y. GadelHak, M. El-Azazy, M.F. Shibl, R.K. Mahmoud, Cost estimation of synthesis and utilization of nano-adsorbents on the laboratory and industrial scales: a detailed review, Sci. Total Environ. 875 (2023), https://doi.org/10.1016/j.scitotenv.2023.162629.
[74] T.M. Mogashane, J.P. Maree, M. Mujuru, M.M. Mphahlele-Makgwane, Technologies that can be Used for the Treatment of Wastewater and Brine for the Recovery of Drinking Water and Saleable Products, in: Recover. Byprod. from Acid Mine Drain. Treat., 2020: pp. 97–156. Doi: 10.1002/9781119620204.ch5.
[75] R. Ragadhita, A.B.D. Nandiyanto, A.C. Maulana, R. Oktiani, A. Sukmafitri, A. Machmud, E.K.A. Surachman, Techo-economic analysis for the production of titanium dioxide nanoparticle produced by liquid-phase synthesis method, J. Eng. Sci. Technol. 14 (2019) 1639–1652.
[76] P. Seferlis, P.S. Varbanov, A.I. Papadopoulos, H.H. Chin, J.J. Klemeš, Sustainable design, integration, and operation for energy high-performance process systems, Energy 224 (2021), https://doi.org/10.1016/j.energy.2021.120158.
[77] M. Arnaboldi, G. Azzone, M. Giorgino, Long- and Short-Term Decision making, Perform. Meas. Manag. Eng. (2015) 107–115, https://doi.org/10.1016/b978-0-12-801902-3.00007-4.
[78] T. Tesfaye, M. Ayele, E. Ferede, M. Gibril, F. Kong, B. Sithole, A techno-economic feasibility of a process for extraction of starch from waste avocado seeds, Clean Technol. Environ, Policy 23 (2021) 581–595, https://doi.org/10.1007/s10098-020-01981-1.